Self-Consistent Simulations of ICRH in Tokamaks and Stellarators

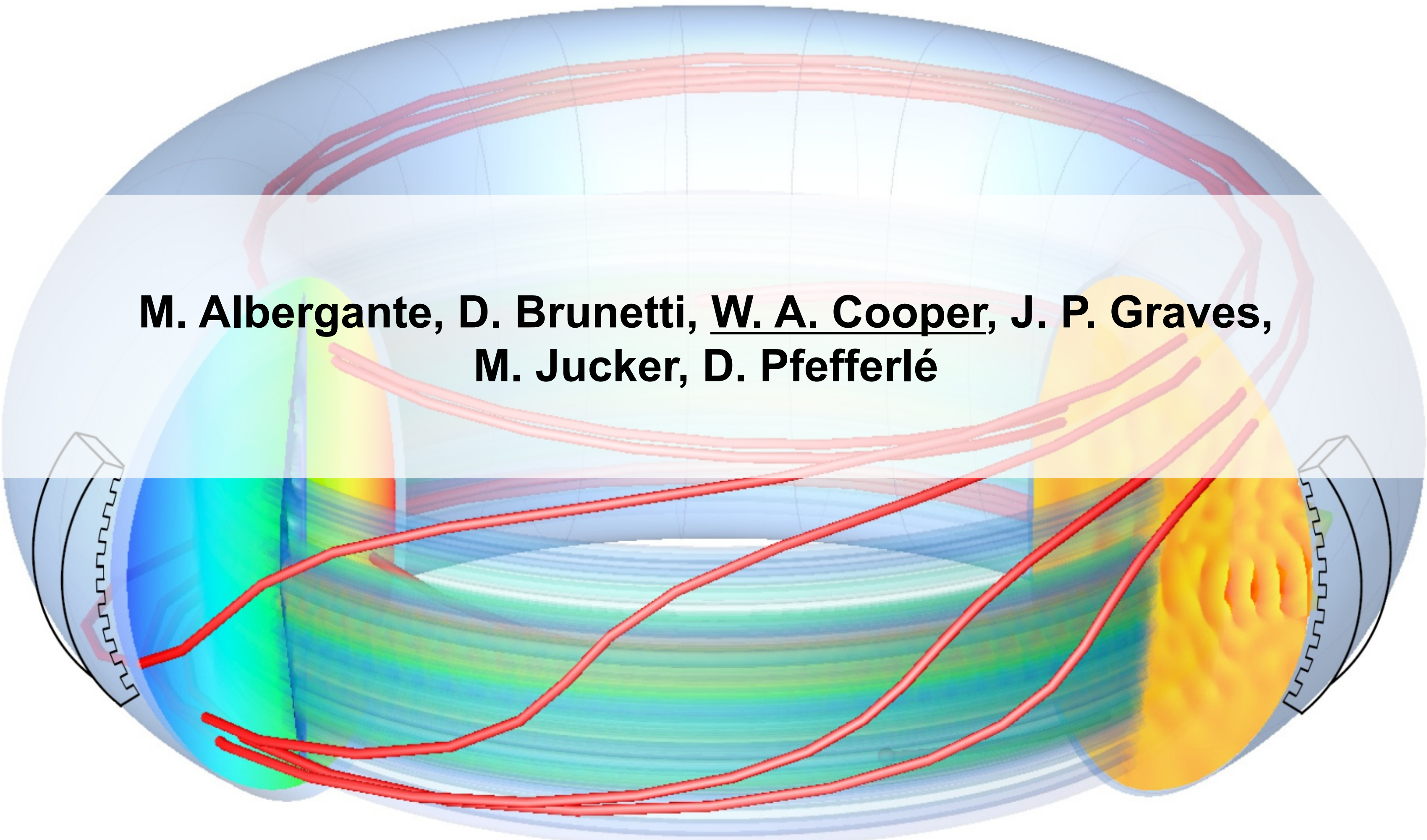

M. Albergante, D. Brunetti, W. A. Cooper, J. P. Graves,
M. Jucker, D. Pfefferlé

ITER International School, Ahmedabad, India, December 2012

Outline

- 1. Introduction
  - Fusion, tokamaks and MHD
  - Suprathermal (fast) particles and impact of heating methods
- 2. Parallelisation of codes calculating fast ion populations
  - Neutral beam injection
  - Ion cyclotron resonance heating
- 3. Description of the SCENIC integrated modeling package
- 4. Applications to JET and a 3D stellarator
- 5. Impact of modelling on fusion experiments
- Conclusions

ITER: next step fusion reactor

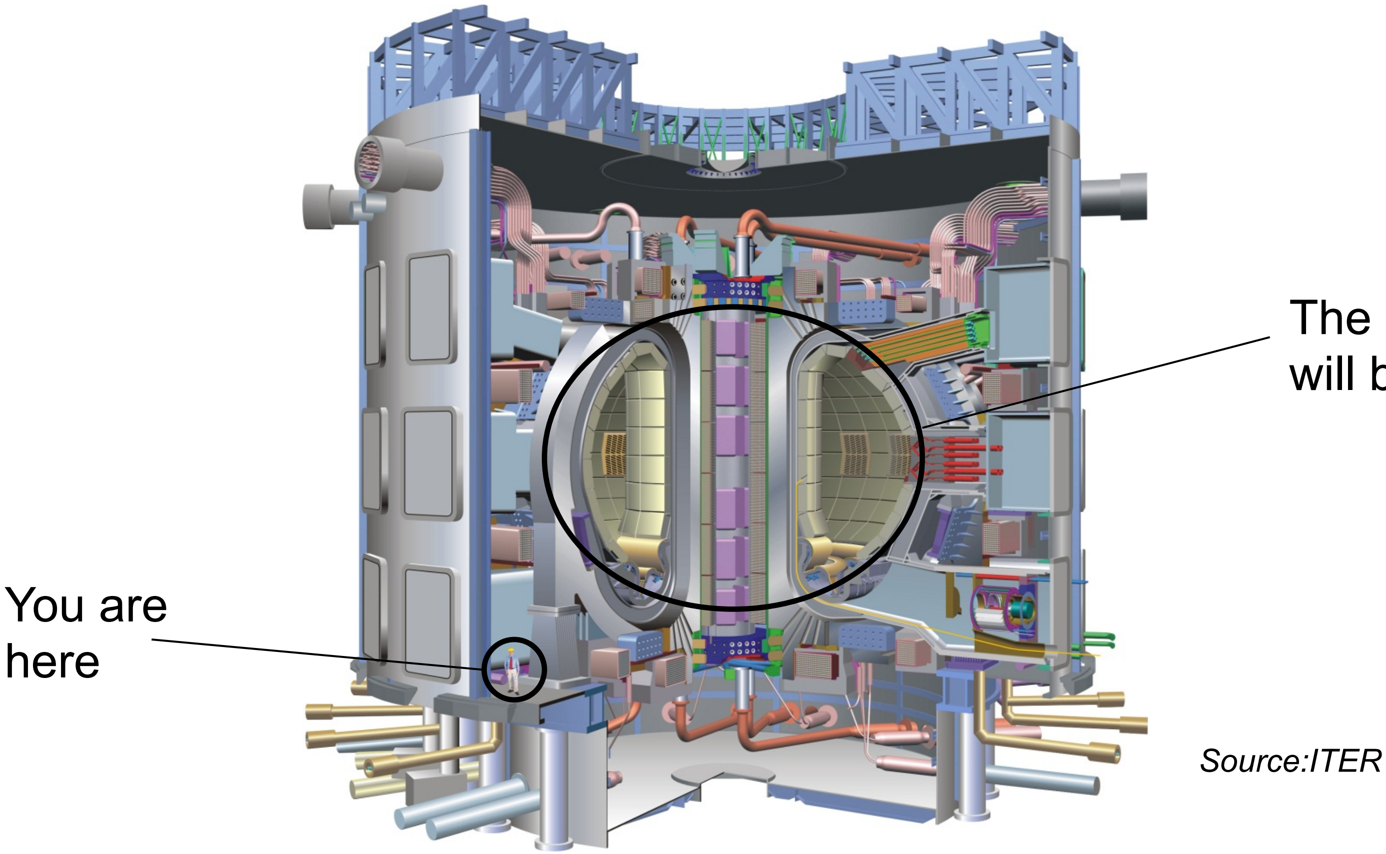

- EU+CH, Japan, USA, China, India, South Korea, Russia
- O(10G€) construction cost (0.30€ / person / year)

Timescales in the ITER plasma

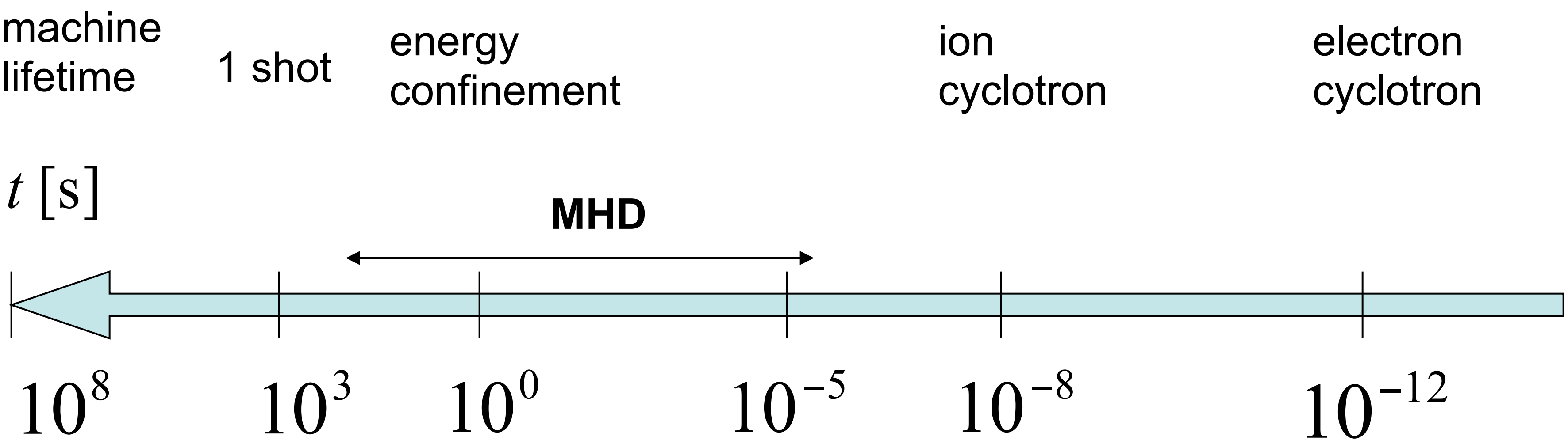

- Physics spans several orders of magnitude
- Direct Numerical Simulation (DNS) of “everything” is unthinkable
  - Need to separate timescales using approximations
  - Our main interest is macroscopic magnetohydrodynamic (MHD) instability, and especially interaction with suprathermal particles.

MHD instability in present day tokamak

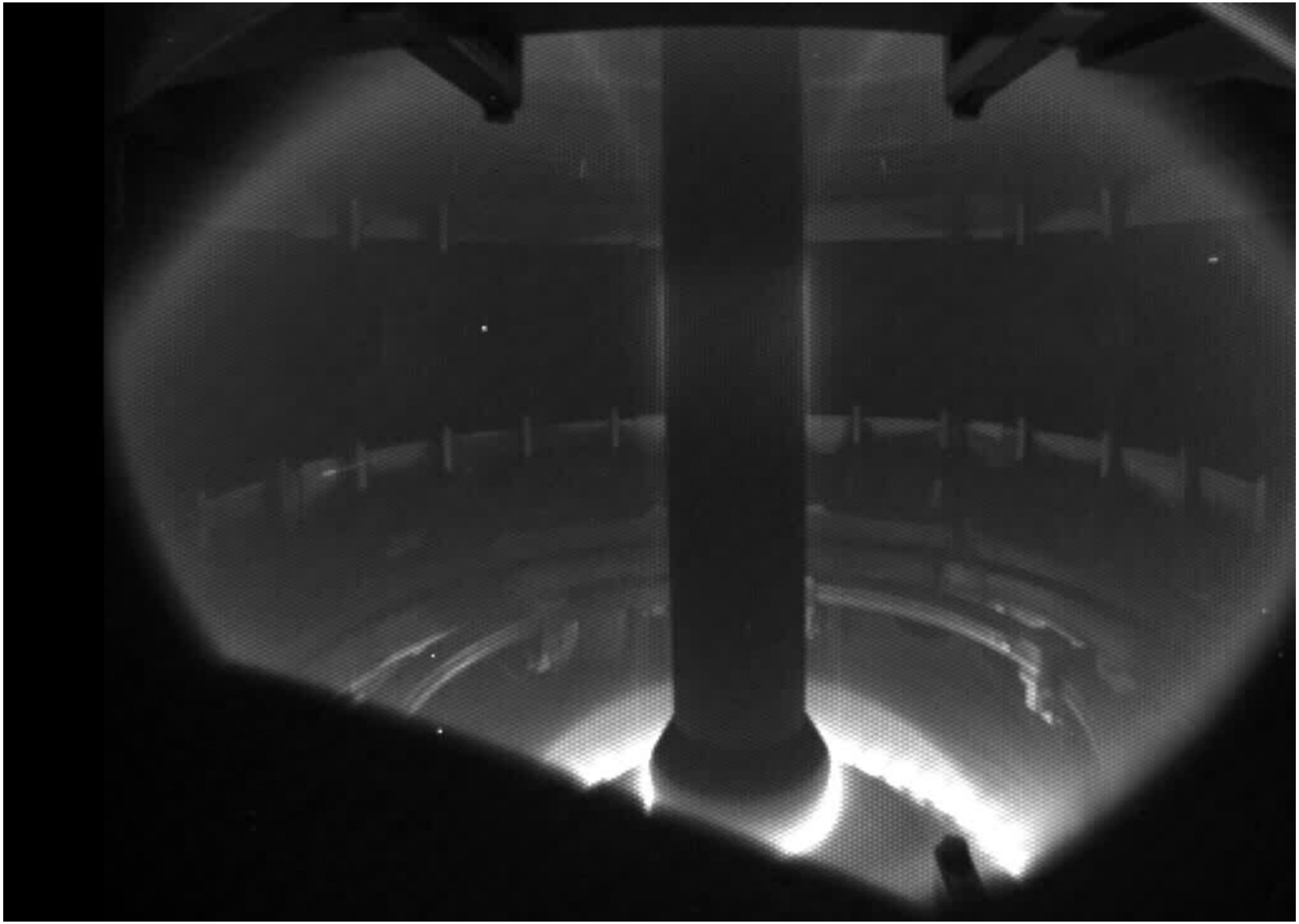

Modelling of such instabilities in TCV tokamak at EPFL

We solve for internal flux surfaces in equilibrium:

- Relax axisymmetry constraint **inside** plasma $$\rho \frac{dV}{dt} = \underline{J} \times \underline{B} - \underline{\nabla} P$$

•A helical MHD plasma state is found [Cooper et al PRL 2010, IAEA proceedings1012]

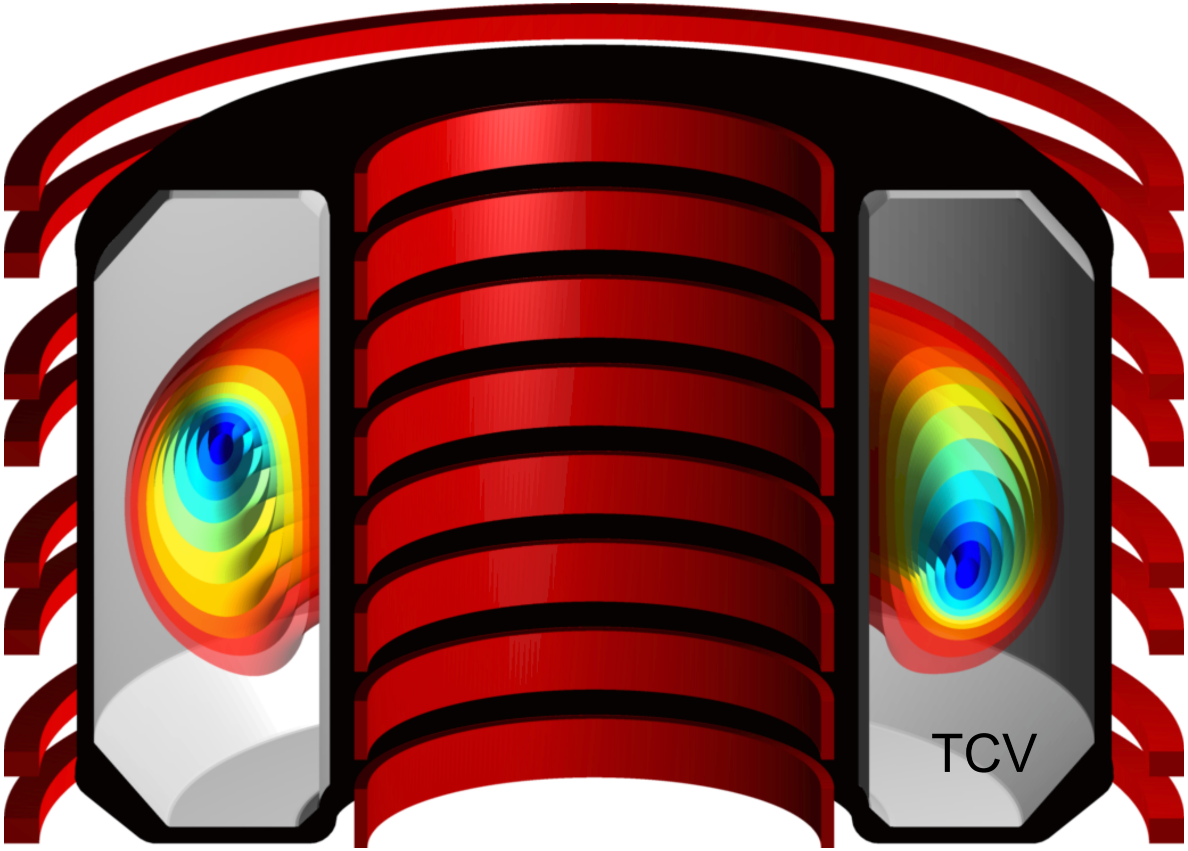

Energetic ion Confinement

Energetic ions are injected in order to heat the plasma by collisions.

Helical instabilities are found to eject the energetic particles and reduce heating efficiency.

No helical instability – Good peaked fast ion density

Strong helical instability – fast ions lost

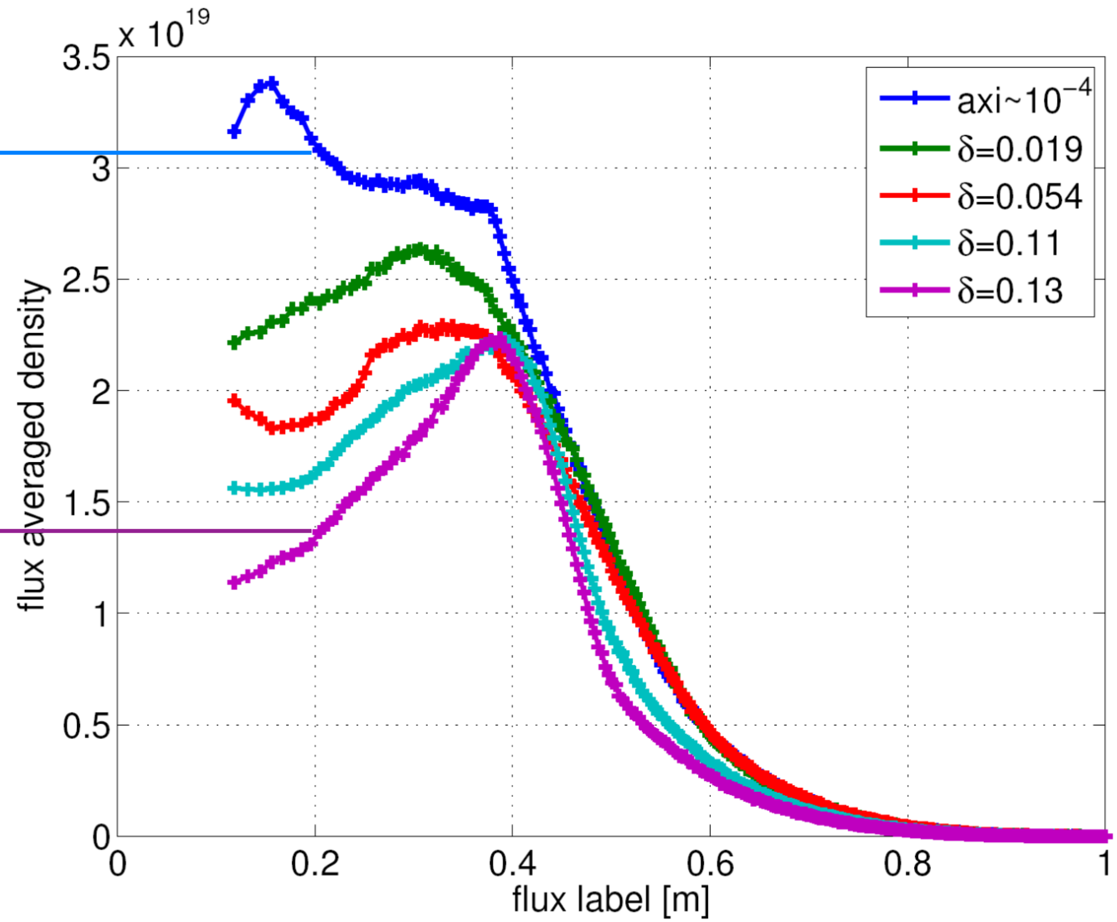

Source: D. Pfefferlé, Varenna Proc. 2012

Energetic ion Confinement

Energetic ions are injected in order to heat the plasma by collisions.

Helical instabilities are found to eject the energetic particles and reduce heating efficiency.

No helical instability – Good peaked fast ion density

Strong helical instability – fast ions lost

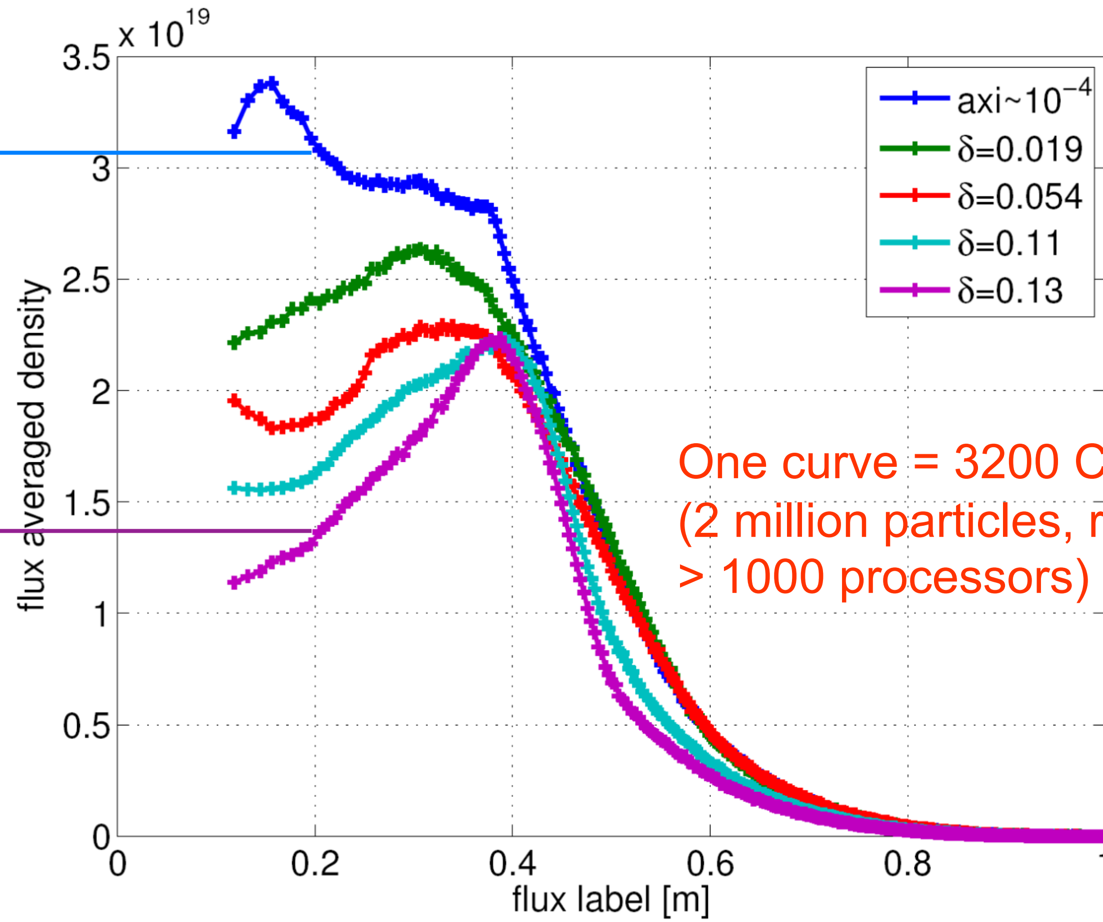

One curve = 3200 CPU-H (2 million particles, run on > 1000 processors)

Source: D. Pfefferlé, Varenna Proc. 2012

Particle orbits in magnetic geometry

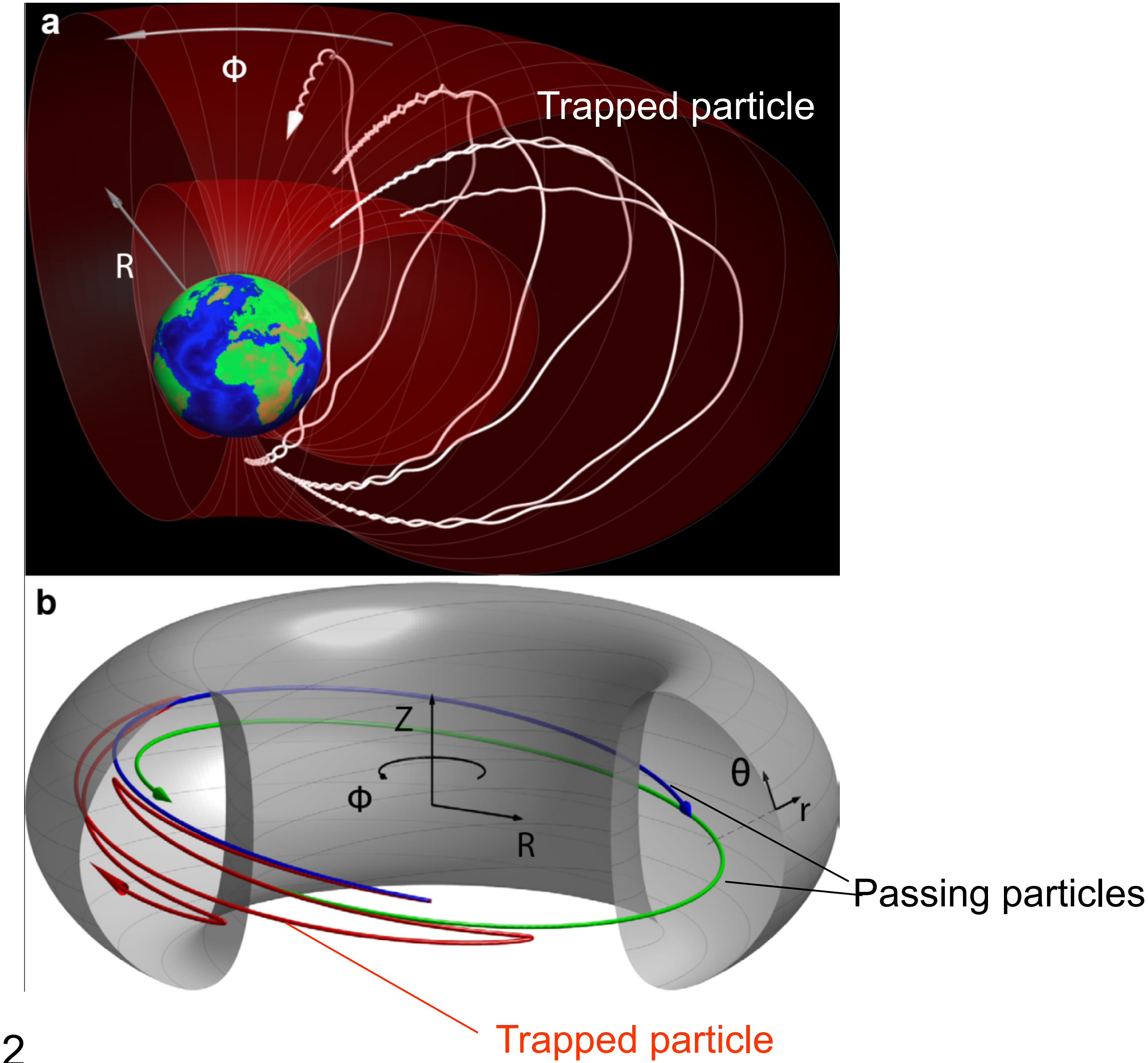

In a tokamak,
two kinds of confined particles exist:
-trapped
-passing

Source: Graves, Nature Commun. 2012

Generation of injected beam population

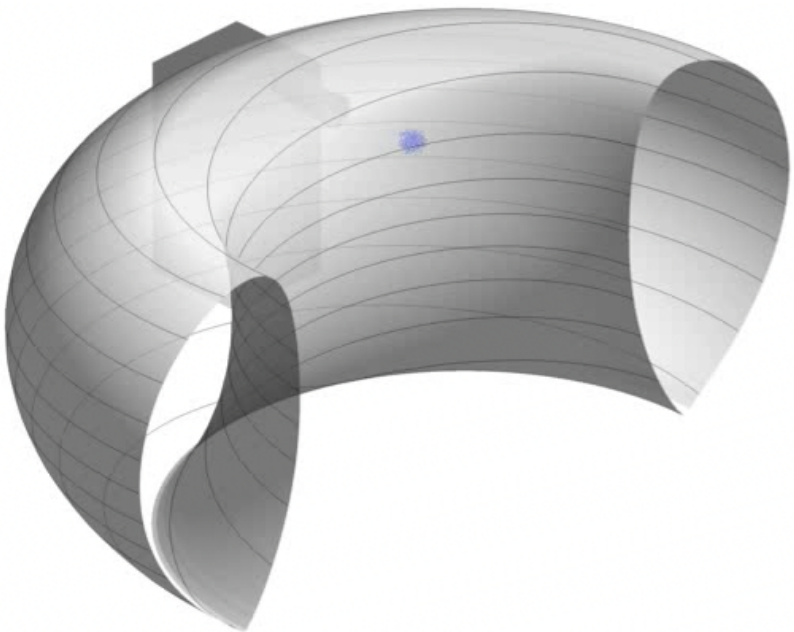

Mattia Albergante

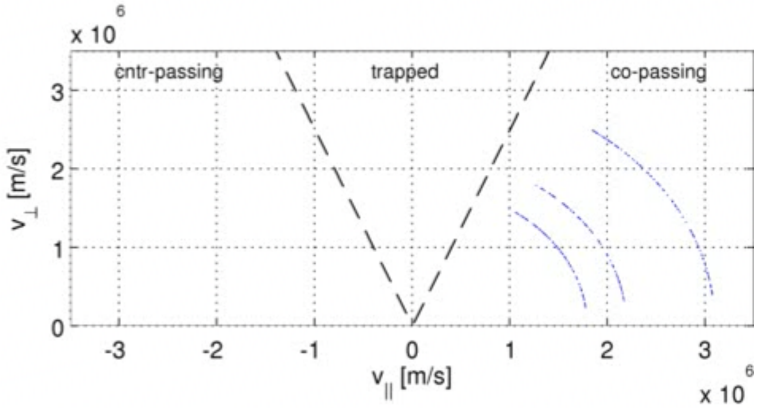

Source: Graves, Nature Commun. 2012

Other Heating Methods in Tokamaks – wave particle resonance

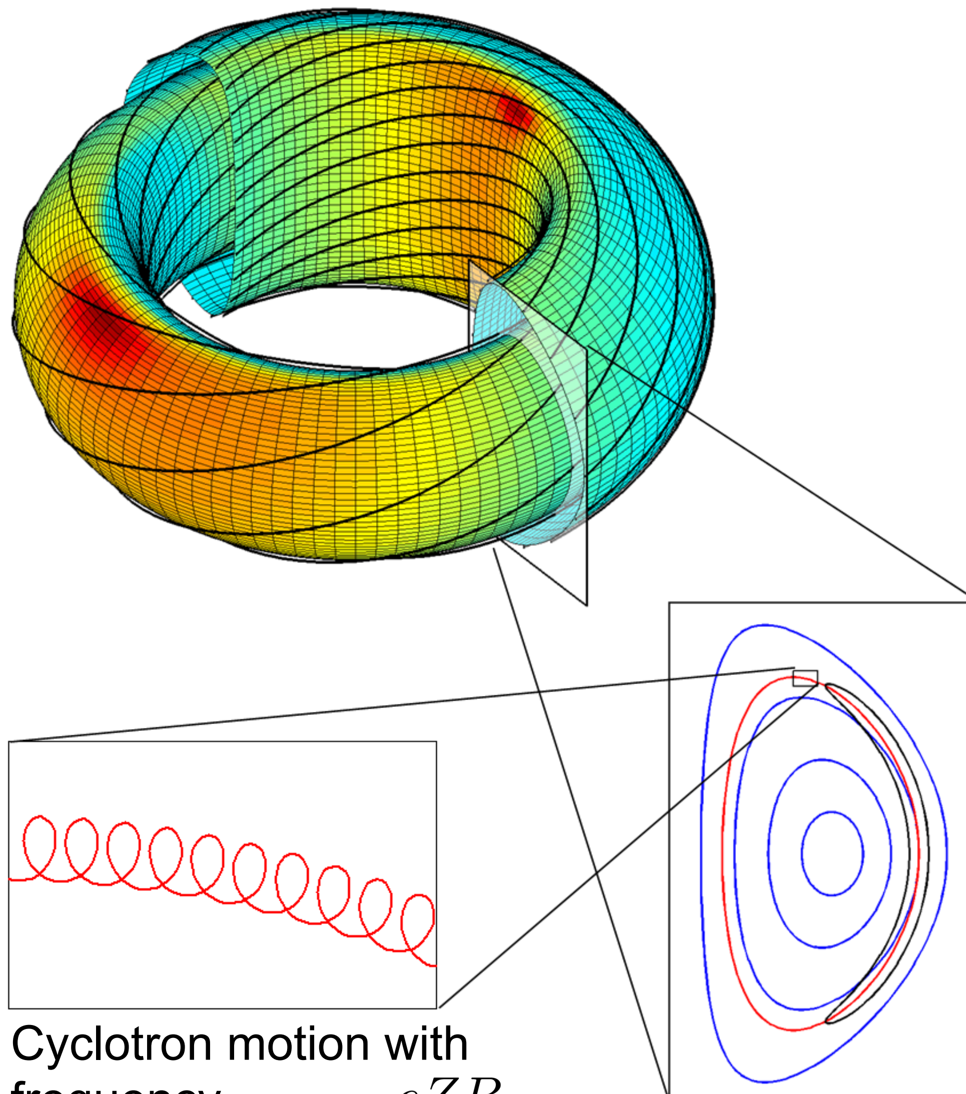

Electron cyclotron heating (ECH)
- microwave injected at electron cyclotron frequency resonates with minority electron population
- hot electrons give up their energy to the plasma via collisions

Ion cyclotron heating (ICRH)
- radio wave injected at ion cyclotron frequency resonates with minority ion population
- hot ions give up their energy to plasma via collisions

Cyclotron motion with frequency $\omega_c = \dfrac{eZB}{M}$

Ion Cyclotron Resonance Heating- wave-particle interaction

Surfers with velocity too different from the phase velocity of the wave will not ride the wave

Surfers with velocity just below the phase velocity of the wave will be accelerated

-> momentum and energy transfer

- General: distribution function in 6D phase space $f(\vec{x},\vec{v};t)$
- To be solved with consistent electromagnetic fields $\vec{E}(\vec{x},t), \vec{B}(\vec{x},t)$

The SCENIC Integrated ICRH Modeling Package

- Self-consistent computation of the MHD equilibrium state, ICRH heating deposition and fast ion distribution in 2D and 3D toroidal plasmas.
- MHD equilibrium computed with the VMEC/ANIMEC code. 3D anisotropic pressure based on a Bi-Maxwellian fast ion distribution function. Nested magnetic flux surfaces.
- ICRH power deposition computed with the LEMan code. Zero order in Larmor radius expansion in 3D Boozer coordinates. Appropriate for minority heating method. Dielectric tensor adapted to bi-Maxwellian fast particle model.
- Guiding centre particle orbits followed with the VENUS code. Anisotropy and relativistic corrections included in the formulation.

Ion Cyclotron Resonance Heating using EPFL SCENIC code

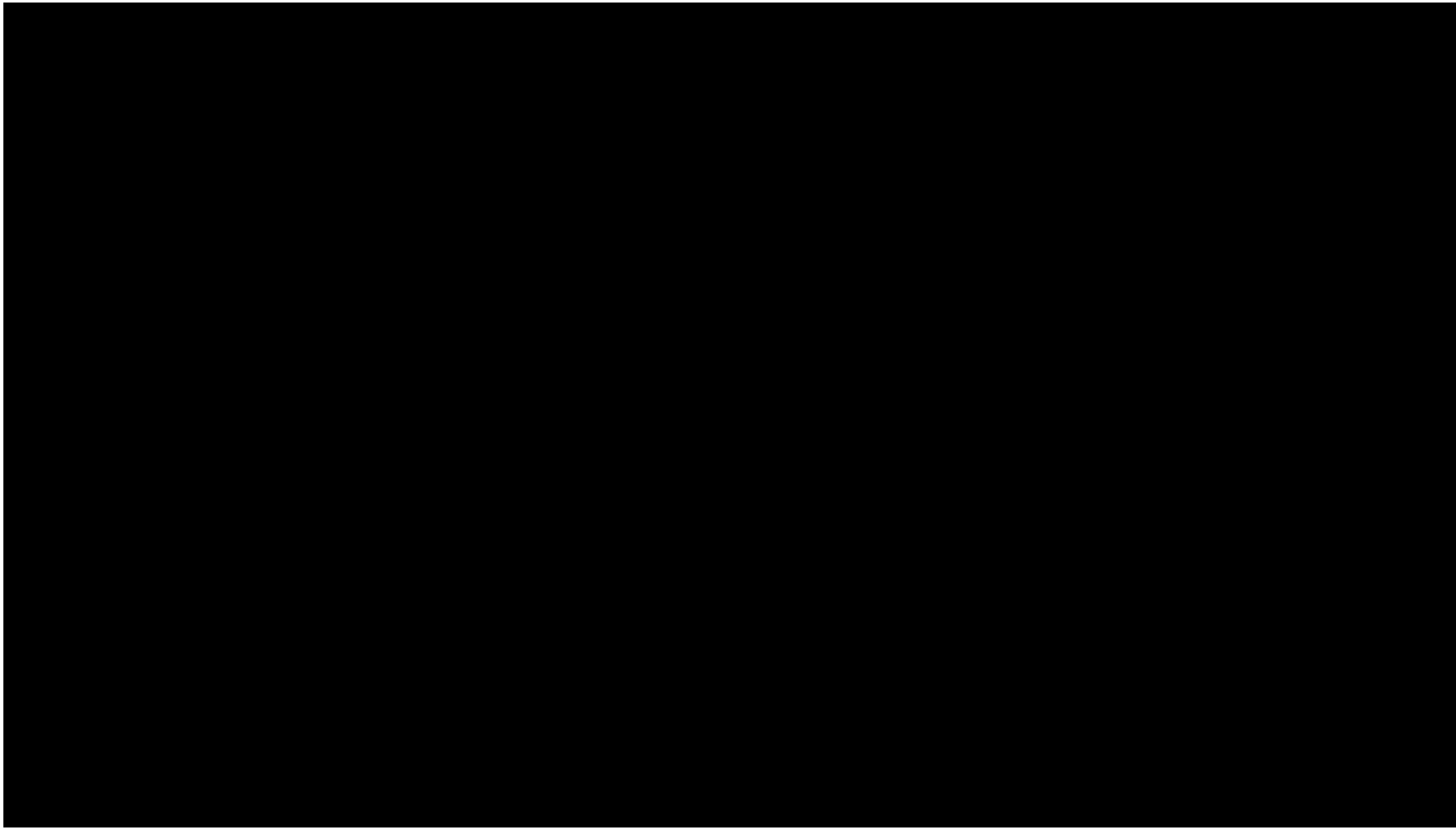

Ion Cyclotron Resonance Heating using EPFL SCENIC code

SCENIC: Self-Consistent Ion Cyclotron

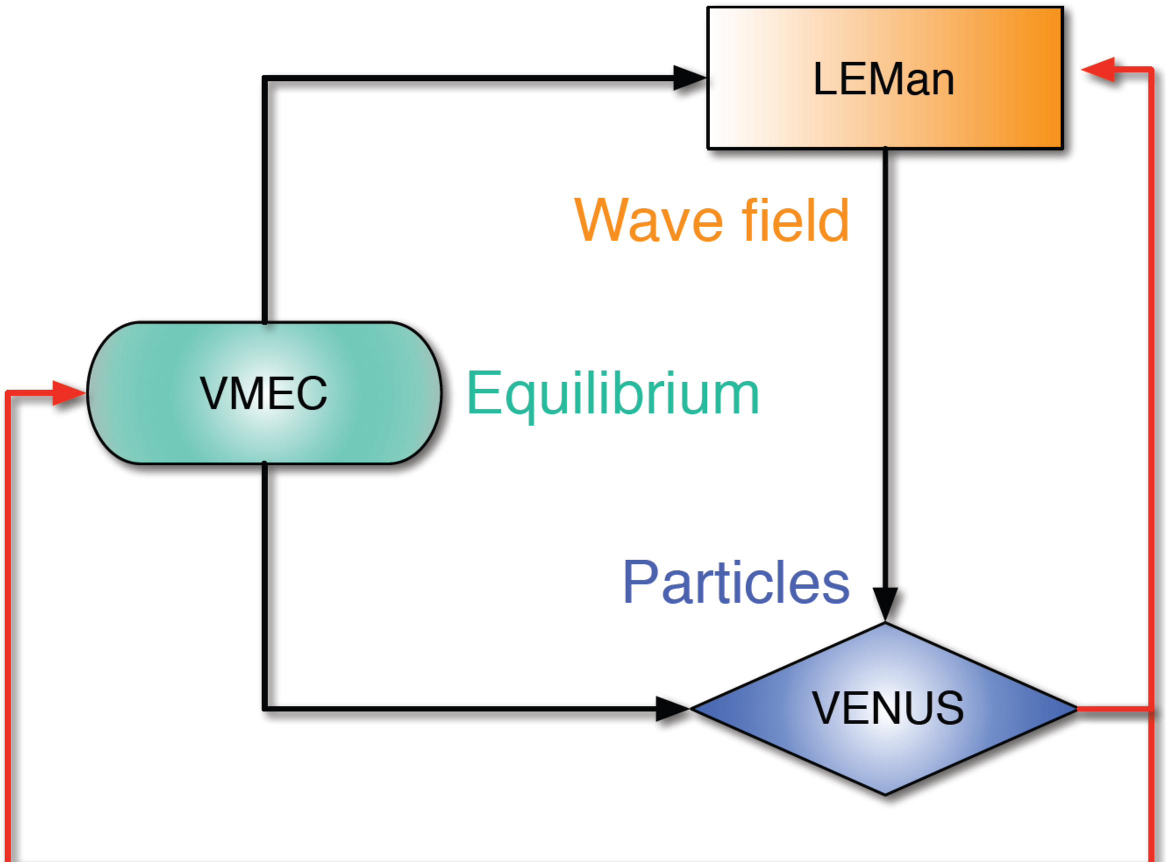

1 iteration $\longrightarrow$ iterated scheme

source: Jucker, EPFL thesis 2010

Ion Cyclotron Resonance Heating using EPFL SCENIC code

SCENIC: Self-Consistent Ion Cyclotron

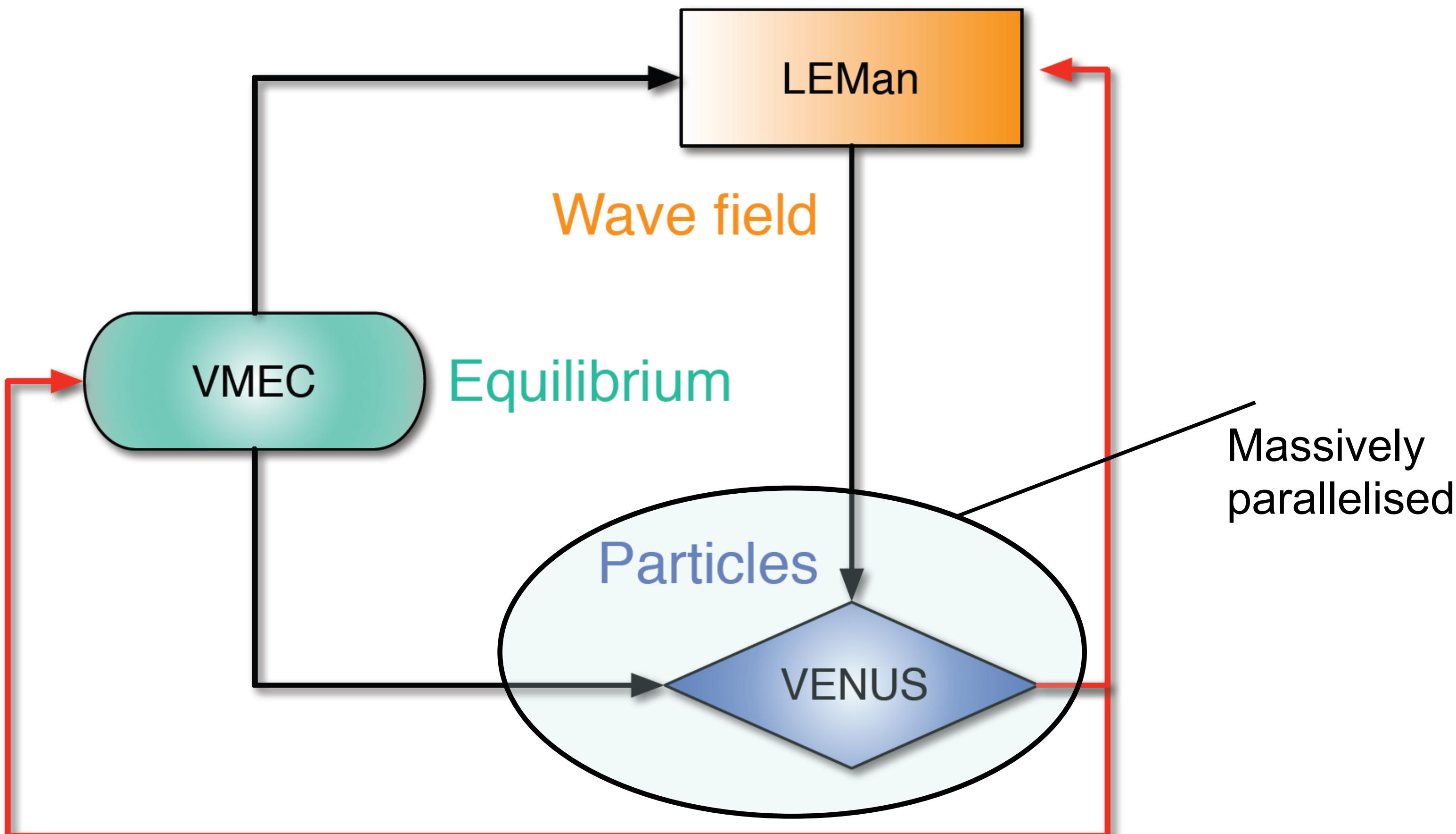

1 iteration $\longrightarrow$ iterated scheme

The Bi-Maxwellian Distribution Function

$$F_h(s,E,\mu) = \mathcal{N}(s)\left(\frac{m}{2\pi T_\perp(s)}\right)^{3/2} \exp\left[-\frac{\mu B_C}{T_\perp(s)} - \frac{|E-\mu B_C|}{T_{||}(s)}\right]$$

- The parallel pressure moment

$$p_{||}(s,B) = p(s) + \mathcal{N}(s) T_{||}(s) H(s,B)$$

- The hot pressure variation factor on a surface for $B \geq B_C$

$$H(s,B) = \frac{\frac{B}{B_C}}{\left[1 - \frac{T_\perp}{T_{||}}\left(1 - \frac{B}{B_C}\right)\right]}$$

- The hot pressure variation factor on a surface for $B < B_C$

$$H(s,B) = \frac{B}{B_C} \frac{\left[1 + \frac{T_\perp}{T_{||}}\left(1 - \frac{B}{B_C}\right) - 2\left(\frac{T_\perp}{T_{||}}\right)^{5/2}\left(1 - \frac{B}{B_C}\right)^{5/2}\right]}{\left[1 - \left(\frac{T_\perp}{T_{||}}\right)\left(1 - \frac{B}{B_C}\right)\right]\left[1 + \left(\frac{T_\perp}{T_{||}}\right)\left(1 - \frac{B}{B_C}\right)\right]}$$

3D Anisotropic Pressure Equilibrium

- The Plasma Energy

$$W = \int\int\int d^3x \left(\frac{B^2}{2\mu_0} + \frac{p_{||}(s,B)}{\Gamma - 1} \right)$$

- The Parallel Pressure

$$p_{||}(s,B) = \mathcal{M}(s)[\Phi'(s)]^{\Gamma} \frac{1 + p_h(s)H(s,B)}{\langle 1 + p_h(s)H(s,B) \rangle^{\Gamma}}$$

- Identify $p(s)p_h(s) = \mathcal{N}(s)T_{||}(s)$ to reconcile hot parallel pressure with Bi-Maxwellian description

- Vary W with respect to t. In equilibrium

$$\frac{dW}{dt} = 0$$

Energy Minimisation

- Solve inverse equilibrium problem: $R = R(s,u,v)$, $Z = Z(s,u,v)$
- s : radial variable, u : poloidal angle, v : toroidal angle

$$\frac{dW}{dt} = - \int\int\int dsdudv \Big[F_R \frac{\partial R}{\partial t} + F_Z \frac{\partial Z}{\partial t} + F_\lambda \frac{\partial \lambda}{\partial t}\Big]$$
$$- \int\int_{s=1} dudv \Big[R\Big(p_\perp + \frac{B^2}{2\mu_0}\Big)\Big(\frac{\partial R}{\partial u}\frac{\partial Z}{\partial t} - \frac{\partial Z}{\partial u}\frac{\partial R}{\partial t}\Big)\Big]$$

- Satisfy firehose and mirror stability criteria

$$\sigma = \frac{1}{\mu_0} - \frac{p_{||} - p_\perp}{B^2} = \frac{1}{\mu_0} - \frac{1}{B}\frac{\partial p_{||}}{\partial B}\Big|_s > 0$$
$$\tau = \frac{1}{\mu_0} + \frac{1}{B}\frac{\partial p_\perp}{\partial B}\Big|_s > 0$$

MHD Forces

- Horizontal Force

$$F_R = \frac{\partial}{\partial u}\left[\sigma\sqrt{g}B^u(\boldsymbol{B}\cdot\boldsymbol{\nabla}R)\right] + \frac{\partial}{\partial v}\left[\sigma\sqrt{g}B^v(\boldsymbol{B}\cdot\boldsymbol{\nabla}R)\right]$$
$$- \frac{\partial}{\partial u}\left[R\frac{\partial Z}{\partial s}\left(p_\perp + \frac{B^2}{2\mu_0}\right)\right] + \frac{\partial}{\partial s}\left[R\frac{\partial Z}{\partial u}\left(p_\perp + \frac{B^2}{2\mu_0}\right)\right]$$
$$+ \frac{\sqrt{g}}{R}\left[\left(p_\perp + \frac{B^2}{2\mu_0}\right) - \sigma R^2(B^v)^2\right]$$

- Vertical Force

$$F_Z = \frac{\partial}{\partial u}\left[\sigma\sqrt{g}B^u(\boldsymbol{B}\cdot\boldsymbol{\nabla}Z)\right] + \frac{\partial}{\partial v}\left[\sigma\sqrt{g}B^v(\boldsymbol{B}\cdot\boldsymbol{\nabla}Z)\right]$$
$$+ \frac{\partial}{\partial u}\left[R\frac{\partial R}{\partial s}\left(p_\perp + \frac{B^2}{2\mu_0}\right)\right] - \frac{\partial}{\partial s}\left[R\frac{\partial R}{\partial u}\left(p_\perp + \frac{B^2}{2\mu_0}\right)\right]$$

- Toroidal Force

$$F_\lambda = \Phi'(s)\left[\frac{\partial(\sigma B_v)}{\partial u} - [\frac{\partial(\sigma B_u)}{\partial v}\right]$$

3D MHD equilibrium

- Fourier decomposition in u and v
- Special finite difference in s
- Accelerated steepest descent method
- Matrix preconditioning applied
- Fixed boundary: prescribe last closed surface
- Free boundary: position and currents in all coils
- Inputs: profiles for p, p_h, $T_\perp/T_{||}$ and $2\pi J$ as a function of s
- Radial force balance diagnostic

$$\left\langle \frac{F_s}{\Phi'(s)} \right\rangle = \left\langle \frac{1}{\Phi'(s)} \frac{\partial p_{||}}{\partial s}\bigg|_B \right\rangle - \frac{\partial}{\partial s}\left\langle \frac{\sigma B_v}{\sqrt{g}} \right\rangle - \iota(s)\frac{\partial}{\partial s}\left\langle \frac{\sigma B_u}{\sqrt{g}} \right\rangle$$

- In 2D, this is the flux surface averaged Grad-Shafranov equation

The Link between ANIMEC and LEMan

- The ANIMEC code is an anisotropic pressure extension of the VMEC code based on the description above.
- VMEC: S.P. Hirshman, O. Betancourt, J. Comput. Phys. **96** (1991) 99; ANIMEC: W.A. Cooper, S.P. Hirshman et al., Comput. Phys. Commun. **180** (2009) 1524.
- The TERPSICHORE code modules that transform equilibrium quantities to Boozer coordinates is applied to generate information for the LEMan ICRH wave propagation code and for the VENUS particle solver.
- The LEMan code solves the Maxwell equations and calculates the power deposition from ICRH waves emitted by an antenna at the edge of the plasma. A direct convolution method and an iterative method used to obtain solutions. The iterative method is preferred for ICRH. (N. Mellet et al, Comput. Phys. Commun. **182** (2011) 570).
- The power absorbed within a flux surface 's' is proportional to:

$$P_{pla}(s) \propto \int_{s<s'} ds' \int d\theta d\phi \boldsymbol{E}^* \cdot \hat{\boldsymbol{\epsilon}} \cdot \boldsymbol{E}$$

The Wave Propagation Equations

- Maxwell's equations

$$\nabla \times \boldsymbol{E} = i\omega \boldsymbol{B} \quad ; \quad \nabla \cdot (\hat{\boldsymbol{\epsilon}} \cdot \boldsymbol{E}) = \rho_{ant}/\epsilon_0;$$
$$\nabla \times \boldsymbol{B} = -i\omega \hat{\boldsymbol{\epsilon}} \cdot \boldsymbol{E} + \mu_0 \boldsymbol{j}_{ant} \quad ; \quad \nabla \cdot \boldsymbol{B} = 0$$

- Electric field formulation

$$\nabla \times (\nabla \times \boldsymbol{E}) - \omega^2 \hat{\boldsymbol{\epsilon}} \cdot \boldsymbol{E} = i\mu_0 \omega \boldsymbol{j}_{ant}$$

- Potential formulation

$$\begin{aligned} \nabla^2 \boldsymbol{A} + \omega^2 \hat{\boldsymbol{\epsilon}} \cdot \boldsymbol{A} + i\omega \hat{\boldsymbol{\epsilon}} \cdot \nabla \Phi_E &= -\mu_0 \boldsymbol{j}_{ant} \\ \nabla \cdot (\hat{\boldsymbol{\epsilon}} \cdot \nabla \Phi_E) - i\omega \nabla \cdot (\hat{\boldsymbol{\epsilon}} \cdot \boldsymbol{A}) &= -\rho_{ant}/\epsilon_0 \end{aligned}$$

- Develop a variational formulation by multiplying with test functions to obtain a weak Galerkin form. In the LEMan code, cubic Hermite finite elements are applied for the radial discretisation and a Fourier decomposition in the Boozer coordinate angular variables is invoked. The Coulomb Gauge $\nabla \cdot \boldsymbol{A} = 0$ is imposed at the boundary. For converged solutions, this condition is satisfied throughout the plasma.

The Bi-Maxwellian Dielectric Tensor

- The dielectric tensor elements for $B \geq B_C$

$$
\begin{aligned}
\mathcal{E}_{nn} &= 1 - \frac{1}{2\omega}\frac{\sqrt{T_{||}/T_{\perp}}}{C_+}\sum_k(\tilde{Z}_1^{||} + \tilde{Z}_{-1}^{||}) \\
\mathcal{E}_{nb} &= -\frac{i}{2\omega}\frac{\sqrt{T_{||}/T_{\perp}}}{C_+}\sum_k(\tilde{Z}_1^{||} - \tilde{Z}_{-1}^{||}) = -\mathcal{E}_{bn} \\
\mathcal{E}_{||} &= 1 + \frac{2}{(k_{||}v_{||t})^2}\frac{\sqrt{T_{||}/T_{\perp}}}{C_+}\sum_k(\tilde{\omega}_p^2 - \omega\tilde{Z}_0^{||})
\end{aligned}
$$

- The dielectric tensor elements for $B < B_C$

$$
\begin{aligned}
\mathcal{E}_{nn} &= \mathcal{E}_{nn}^{B\geq B_C} - \frac{1}{2\omega}\frac{C_+ - C_-}{C_+C_-}\sum_k(\tilde{Z}_1^{\perp} + \tilde{Z}_{-1}^{\perp}) \\
\mathcal{E}_{nb} &= \mathcal{E}_{nb}^{B\geq B_C} - \frac{1}{2\omega}\frac{C_+ - C_-}{C_+C_-}\sum_k(\tilde{Z}_1^{\perp} - \tilde{Z}_{-1}^{\perp}) = -\mathcal{E}_{bn} \\
\mathcal{E}_{||} &= \mathcal{E}_{||}^{B\geq B_C} - \frac{C_+ - C_-}{C_+C_-}\sum_k\left(\sqrt{\frac{B_C - B}{B_C}}\tilde{\omega}_p^2 - \omega\tilde{Z}_0^{\perp}\right)
\end{aligned}
$$

Coefficients in the Dielectric Tensor

- The cyclotron frequency is $\Omega_C = \frac{q_k B_C}{m_k}$; the plasma frequency squared is $\tilde{\omega}_p^2 = \frac{q_k^2 \mathcal{N}}{\epsilon_0 m_k}$ and $v_{||t}^2 = \frac{2T_{||}}{m_k}$.

$$C_{\pm} = \frac{B_C}{B} \pm \frac{T_{\perp}}{T_{||}} \left(1 - \frac{B_C}{B} \right)$$

$$Z^{Sh}(z) = \frac{z}{\sqrt{\pi}} \int_{-\infty}^{+\infty} \frac{1}{z-x} e^{-x^2} dx \qquad ; \qquad Im\ z > 0$$

$$\tilde{Z}_{\ell}^{||} = \frac{\tilde{\omega}_p^2}{\omega - \ell\Omega_C} Z^{Sh} \left(\frac{\omega - \ell\Omega_C}{k_{||} v_{||t}} \right)$$

$$\tilde{Z}_{\ell}^{\perp} = \sqrt{\frac{B_C - B}{B_C}} \frac{\tilde{\omega}_p^2}{\omega - \ell\Omega_C} Z^{Sh} \left(\sqrt{\frac{B_C}{B_C - B}} \frac{\omega - \ell\Omega_C}{k_{||} v_{||t}} \right)$$

Physics Basis of the VENUS Code

- Particle following code in the drift approximation
- Applies 4th order Runge-Kutta scheme to follow individual particle orbits
- Coulomb and RF collision operators implemented
- Specifically the parallel pressure moment of the distribution of particles that are followed is determined and is fitted to the corresponding moment of the bi-Maxwellian fast particle distribution function

Guiding Centre Drift Motion

- The momentum in the drift approximation

The toroidal equation of motion

$$\boldsymbol{P} = P_{||}(\boldsymbol{B}/B) + e\boldsymbol{A}$$

- The parallel gyroradius

$$\rho_{||} = P_{||}/(e\sigma B)$$

- The Lagrangian for the drift motion

$$\mathcal{L}dt = \boldsymbol{P} \cdot d\boldsymbol{x} - \mathcal{H}dt = e(\rho_{||}\sigma\boldsymbol{B} + \boldsymbol{A}) \cdot d\boldsymbol{x} - \mathcal{H}dt$$

- After expansion and manipulation in Boozer coordinates (*R. White, Phys. Fluids B **2** (1990) 845; Cooper et al., PPCF **53** (2011) 024001*), the Lagrangian is

$$\frac{\mathcal{L}dt}{e} = [\Phi(s) + \rho_{||}\mu_0 J(s) + A_\theta]d\theta - [\psi(s) + \rho_{||}\mu_0 I(s) - A_\phi]d\phi + A_s ds - \frac{\mathcal{H}dt}{e}$$

- The Boozer coordinates are canonical for drift motion when the Gauge $A_s = 0$ is imposed.

Hamiltonian drift motion approach

- The canonical momenta are.

$$
\begin{aligned}
P_\phi &= -\psi(s) - \rho_{||}\mu_0 I(s) + A_\phi(s,\theta,\phi,t) \\
P_\theta &= \Phi(s) + \rho_{||}\mu_0 J(s) + A_\theta(s,\theta,\phi,t)
\end{aligned}
$$

- The Hamiltonian for guiding centre drift motion is

$$
\frac{\mathcal{H}}{e} = \gamma m_0 c^2/e + \Phi_E(s,\theta,\phi,t) = \mathcal{H}_e \qquad ; \qquad \gamma = \sqrt{1 + \frac{2\mu B}{m_0 c^2} + \left(\frac{e\sigma B \rho_{||}}{m_0 c}\right)^2}
$$

- The equations of motion from the Hamiltonian formalism are

$$
\begin{aligned}
\dot{P}_\theta &= -\frac{\partial \mathcal{H}_e}{\partial \theta}\bigg|_{P_\theta, P_\phi, \phi, t} \quad ; \quad \dot{\theta} = \frac{\partial \mathcal{H}_e}{\partial P_\theta}\bigg|_{P_\phi, \theta, \phi, t} \\
\dot{P}_\phi &= -\frac{\partial \mathcal{H}_e}{\partial \phi}\bigg|_{P_\theta, P_\phi, \theta, t} \quad ; \quad \dot{\phi} = \frac{\partial \mathcal{H}_e}{\partial P_\phi}\bigg|_{P_\theta, \theta, \phi, t}
\end{aligned}
$$

- It is more convenient to follow particle $\dot{s}$ and $\dot{\rho}_{||}$ rather than the canonical momenta $\dot{P}_\theta$ and $\dot{P}_\phi$

Drift orbit equations of motion

- The radial equation of motion

$$\dot{s} = \frac{1}{\gamma D}\left(\frac{\mu}{e} + \sigma\tau\frac{eB\rho_{||}^2}{m_0}\right)\left[\mu_0 I(s)\frac{\partial B}{\partial\theta} + \mu_0 J(s)\frac{\partial B}{\partial\phi}\right] + \frac{1}{D}\left[\mu_0 I(s)\frac{\partial\Phi_E}{\partial\theta} + \mu_0 J(s)\frac{\partial\Phi_E}{\partial\phi}\right] - \frac{e\sigma^2 B^2\rho_{||}}{\gamma m_0 D}\left(\frac{\partial A_\phi}{\partial\theta} - \frac{\partial A_\theta}{\partial\phi}\right)$$

- The poloidal equation of motion

$$\dot{\theta} = -\frac{\mu_0 I(s)}{\gamma D}\left[\left(\frac{\mu}{e} + \sigma\tau\frac{eB\rho_{||}^2}{m_0}\right)\frac{\partial B}{\partial s} + \frac{e\sigma B^2\rho_{||}^2}{m_0}\left.\frac{\partial\sigma}{\partial s}\right|_B\right] + \frac{e\sigma^2 B^2\rho_{||}}{\gamma m_0 D}\left[\psi'(s) + \mu_0 I'(s)\rho_{||}\right] - \frac{\mu_0 I(s)}{D}\frac{\partial\Phi_E}{\partial s} - \frac{e\sigma^2 B^2\rho_{||}}{\gamma m_0 D}\frac{\partial A_\phi}{\partial s}$$

- The toroidal equation of motion

$$\dot{\phi} = -\frac{\mu_0 J(s)}{\gamma D}\left[\left(\frac{\mu}{e} + \sigma\tau\frac{eB\rho_{||}^2}{m_0}\right)\frac{\partial B}{\partial s} + \frac{e\sigma B^2\rho_{||}^2}{m_0}\left.\frac{\partial\sigma}{\partial s}\right|_B\right] + \frac{e\sigma^2 B^2\rho_{||}}{\gamma m_0 D}\left[\Phi'(s) + \mu_0 J'(s)\rho_{||}\right] - \frac{\mu_0 J(s)}{D}\frac{\partial\Phi_E}{\partial s} + \frac{e\sigma^2 B^2\rho_{||}}{\gamma m_0 D}\frac{\partial A_\theta}{\partial s}$$

ICRH Collision Operators

- Construct Monte Carlo operator to provide random kicks to perpendicular velocity (*Eriksson, Schneider, Phys. Plasmas **12** (2005) 072524*)

$$\Delta v_\perp = \frac{\langle \Delta v_\perp^2 \rangle}{4 v_\perp} + \mathcal{R}\sqrt{2\langle \Delta v_\perp^2 \rangle}$$

$$\sqrt{\langle \Delta v_\perp^2 \rangle} = \tau \frac{e}{m}\left| E^+ \mathcal{J}_{n-1}\left(\frac{k_\perp v_\perp}{\Omega}\right) + E^- \mathcal{J}_{n+1}\left(\frac{k_\perp v_\perp}{\Omega}\right)\right|$$

- The interaction time τ is the phase integral (*T. Johnson et al. Nucl. Fusion **46** (2006) S433*)

$$\tau = \int dt' e^{i\nu} \qquad ; \qquad \nu(t) = \int dt' (\omega - k_{||}v_{||} - n\Omega)$$

- The Monte Carlo operator for the parallel velocity is

$$\Delta v_{||} = \frac{k_{||}}{n\Omega} v_\perp \Delta v_\perp$$

EM Fields link from LEMan to VENUS

- The Electromagnetic Fields in the LEMan code invoke the Coulomb Gauge $\boldsymbol{\nabla} \cdot \boldsymbol{A} = 0$
- The Electromagnetic Fields in the VENUS code apply the Gauge $A_s = 0$ (we define it as the Drift Gauge)
- Any magnetic field derived from the vector potential is invariant to the addition of a gradient of a scalar function. Hence

$$\boldsymbol{A}^{VENUS} + \boldsymbol{\nabla} G = \boldsymbol{A}^{LEMan}$$

- The radial, poloidal and toroidal projections (like $\sqrt{g}\boldsymbol{\nabla}\theta \times \boldsymbol{\nabla}\phi$) of $\boldsymbol{A}$ can be expressed as

$$\begin{aligned}
\frac{\partial G}{\partial s} &= A_s^{LEMan} \\
A_\theta^{VENUS} &= A_\theta^{LEMan} - \frac{\partial G}{\partial \theta} \\
A_\phi^{VENUS} &= A_\phi^{LEMan} - \frac{\partial G}{\partial \phi}
\end{aligned}$$

- The electrostatic potential is obtained from Faraday's Law ($\boldsymbol{E} = -\boldsymbol{\nabla}\Phi_E - \partial \boldsymbol{A}/\partial t$). This allows us to express:

$$\frac{\partial \Phi_E^{VENUS}}{\partial \theta} = \frac{\partial \Phi_E^{LEMan}}{\partial \theta} - \frac{\partial A_\theta^{VENUS}}{\partial t} + \frac{\partial A_\theta^{LEMan}}{\partial t}$$

The Wave Numbers in VENUS

- The standard approximation for axisymmetric tokamaks is to impose $k_{||} = n_\phi / R$. This is very simple to implement, but becomes inadequate in 3D magnetic confinement configurations. Instead, the wave numbers are obtained from the scalar potential Φ_E.

$$|k_{||}| = \left| \frac{1}{\Phi_E \sqrt{g} B} \left[\psi'(s) \frac{\partial \Phi_E}{\partial \theta} + \Phi'(s) \frac{\partial \Phi_E}{\partial \phi} \right] \right|$$

$$|k_\perp|^2 = \left| (\boldsymbol{\nabla} s \cdot \boldsymbol{\nabla} s) \left(\frac{1}{\Phi_E} \frac{\partial \Phi_E}{\partial s} \right) \right|^2 + \left| \frac{1}{(\boldsymbol{\nabla} s \cdot \boldsymbol{\nabla} s)} \frac{1}{\sigma \sqrt{g} B \Phi_E} \left[\mu_0 I(s) \frac{\partial \Phi_E}{\partial \theta} + \mu_0 J(s) \frac{\partial \Phi_E}{\partial \phi} \right] \right|^2$$

- Further details about SCENIC:
  M. Jucker et al., Comput. Phys Commun. ***182*** *(2011) 812*
  M. Jucker et al., PPCF ***53*** *(2011) 054010*
  M. Jucker et al., Nucl. Fusion ***52*** *(2012) 013015*

Ion Cyclotron Resonance Heating – Over 1 million markers followed

Between iterations, the particle population does not modify the electromagnetic wave, nor impact on the magnetic equilibrium

Moreover, the particles do not interact with each other between iterations.

Hence, the population statistics for the marker trajectories and their cumulative distribution in real space and velocity space is trivially parallelisable using MPI (between iterations.).

At the end of one iteration the wave field and equilibrium are updated. This is not parallelised, but the time required for this is very small.

Ion Cyclotron Resonance Heating – Over 1 million markers followed

The population statistics for the marker trajectories and their cumulative distribution in real space and velocity space is trivially parallelisable (between iterations.).

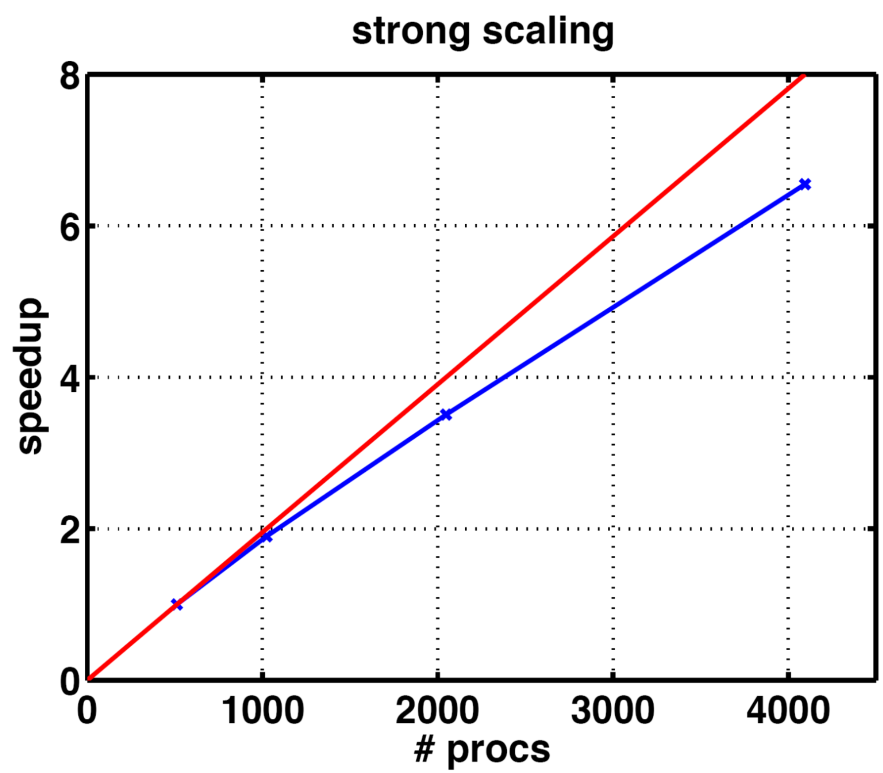

source: Jucker, EPFL thesis 2010

Ion Cyclotron Resonance Heating

At the end of one iteration the wave field and equilibrium are updated. This is not parallelised, but the time required for this is very small.

Moreover, very few iterations are required in practice.

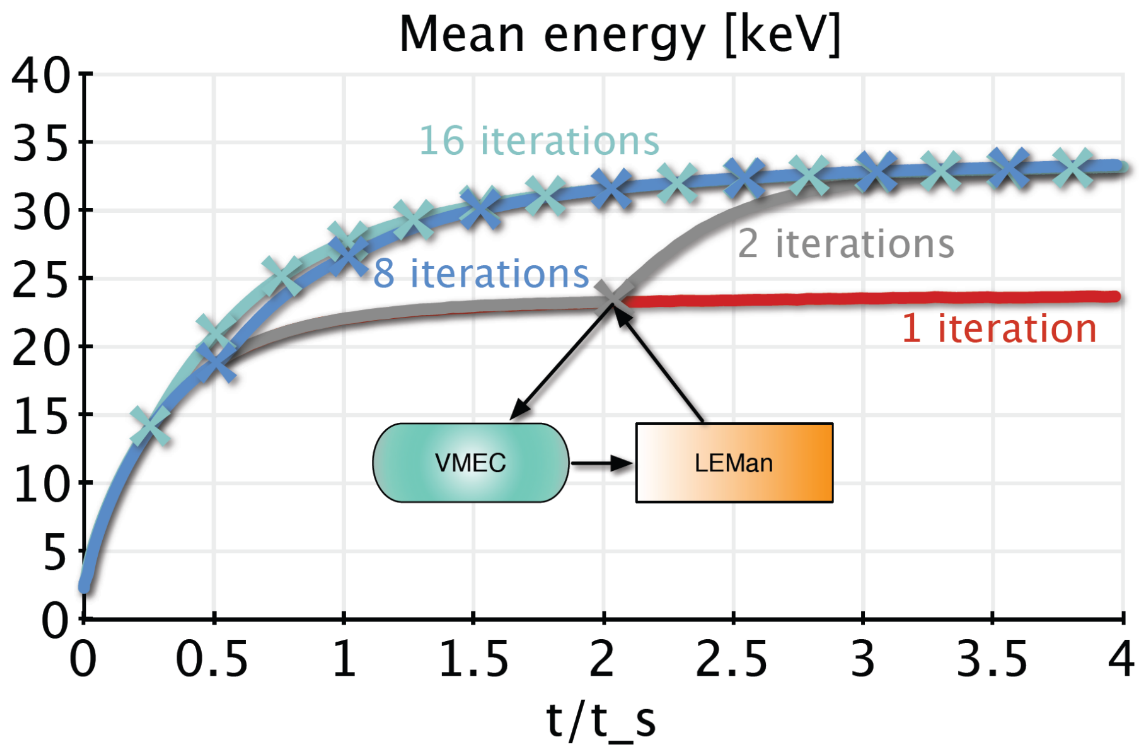

source: Jucker, EPFL thesis 2010

Generation of hot ion population between iterations – massively parallelised

VENUS

Change to equilibrium pressure (magnetic field) and wave at each iteration

LEMan

VMEC

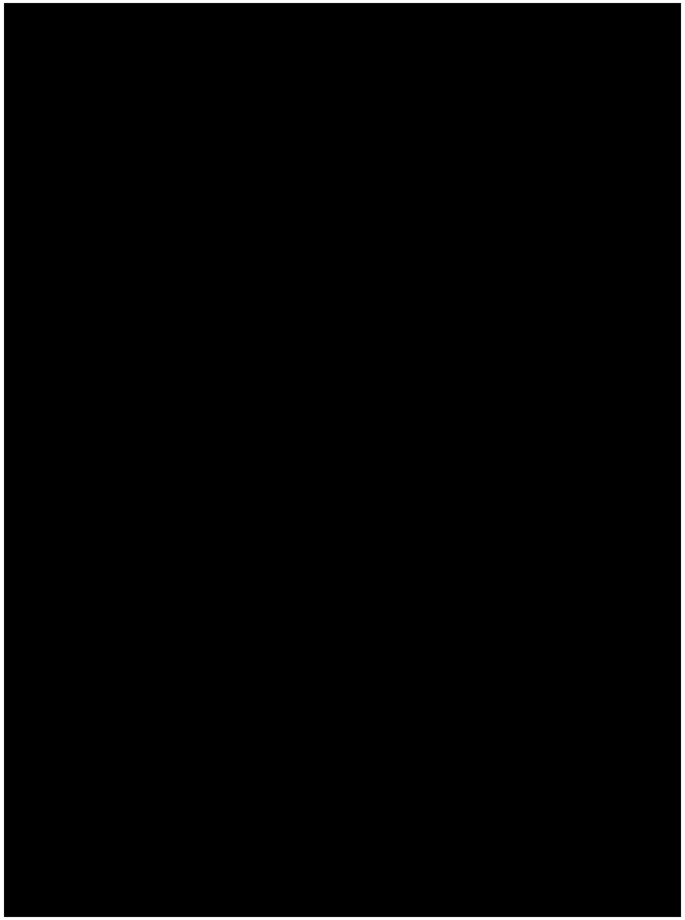

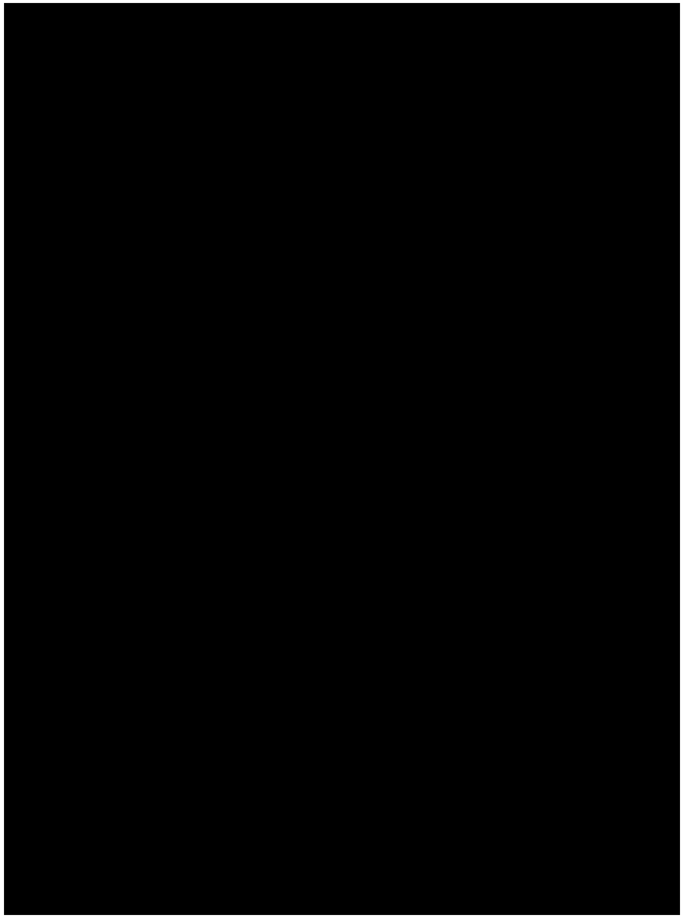

SCENIC ICRH Simulation in a Quasi-Axisymmetric Stellarator

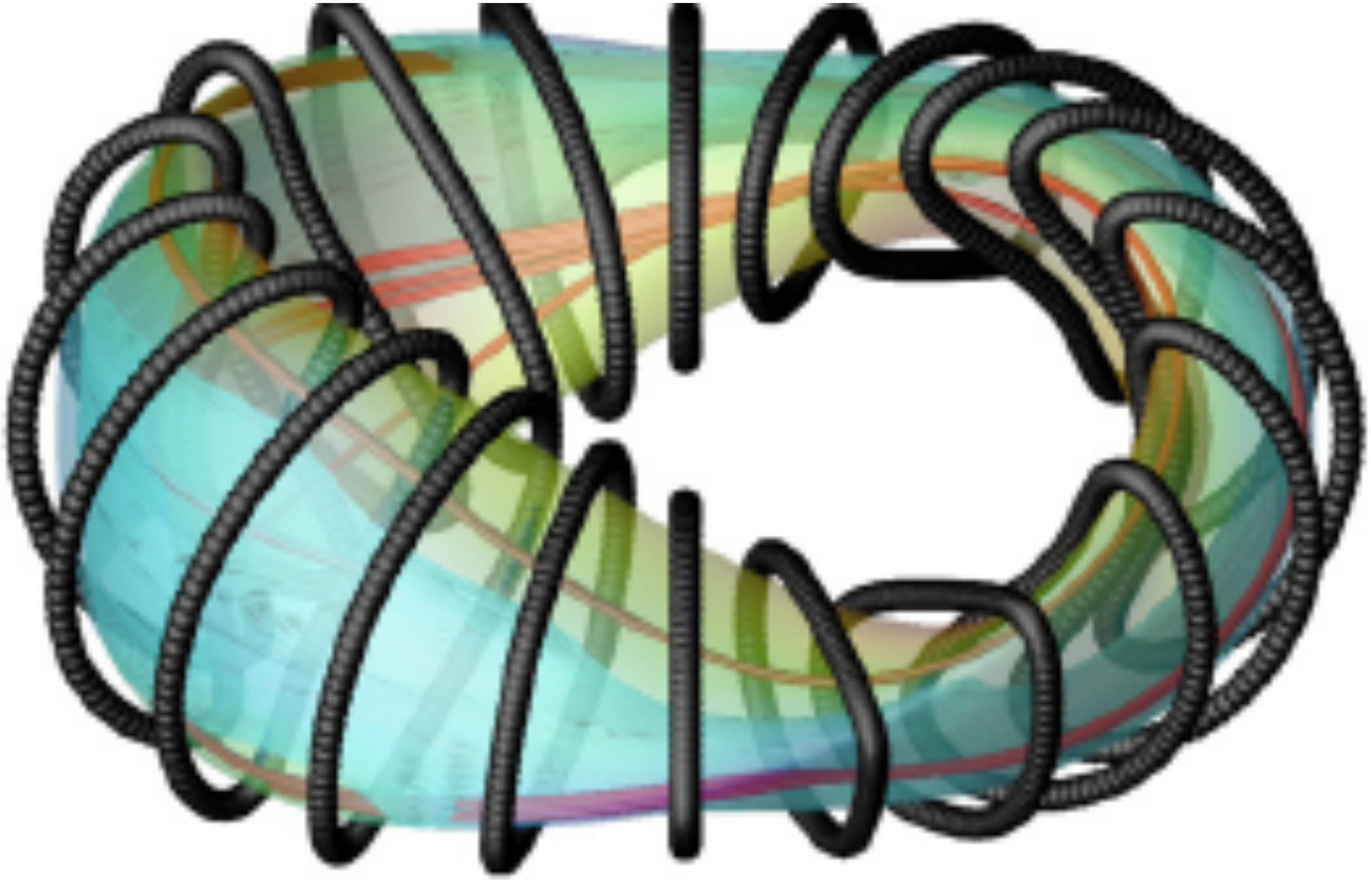

- source: M. Jucker *et al.*, Nucl. Fusion **52** (2012) 013015

Quasi-Axisymmetric Stellarator ICRH

- ANIMEC mod-B
- LEMan Power Deposition
- VENUS power deposition

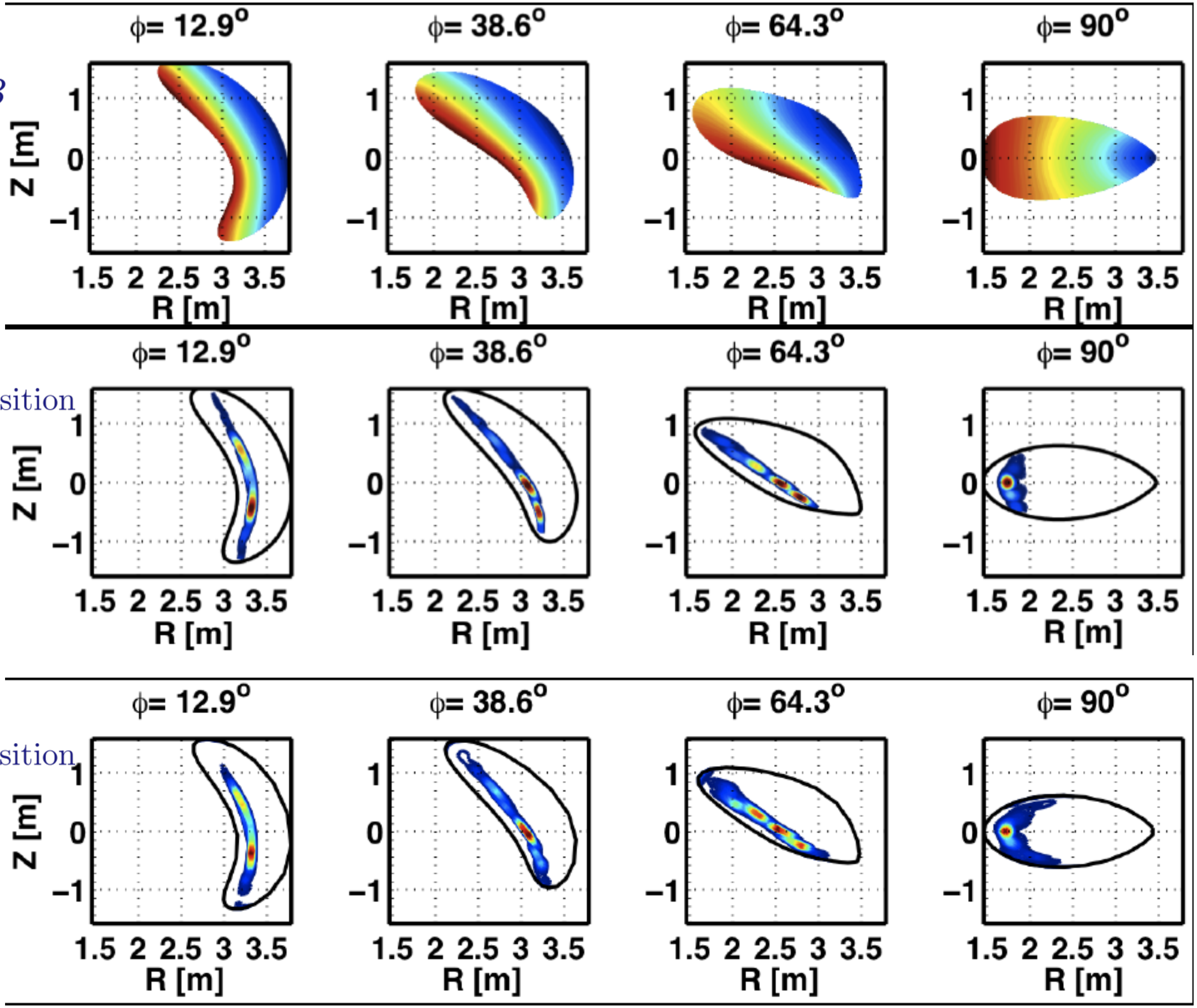

Hot Particle Pressure from ICRH in a Quasi-Axisymmetric Stellarator

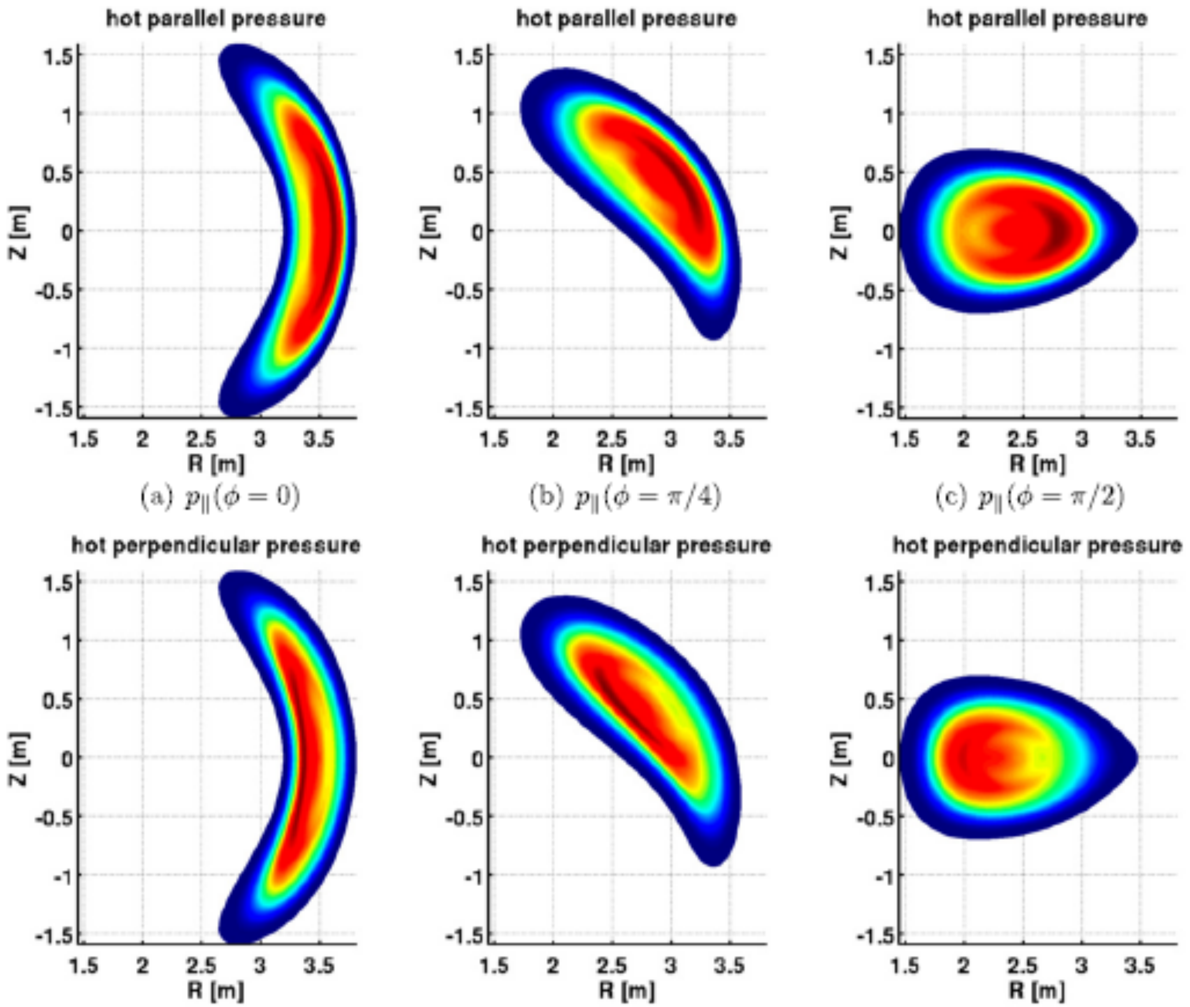

(a) $p_{\parallel}(\phi = 0)$ (b) $p_{\parallel}(\phi = \pi/4)$ (c) $p_{\parallel}(\phi = \pi/2)$

(d) $p_{\perp}(\phi = 0)$ (e) $p_{\perp}(\phi = \pi/4)$ (f) $p_{\perp}(\phi = \pi/2)$

Hot Particle Perpendicular Pressure in 2-Field Period QAS from VENUS

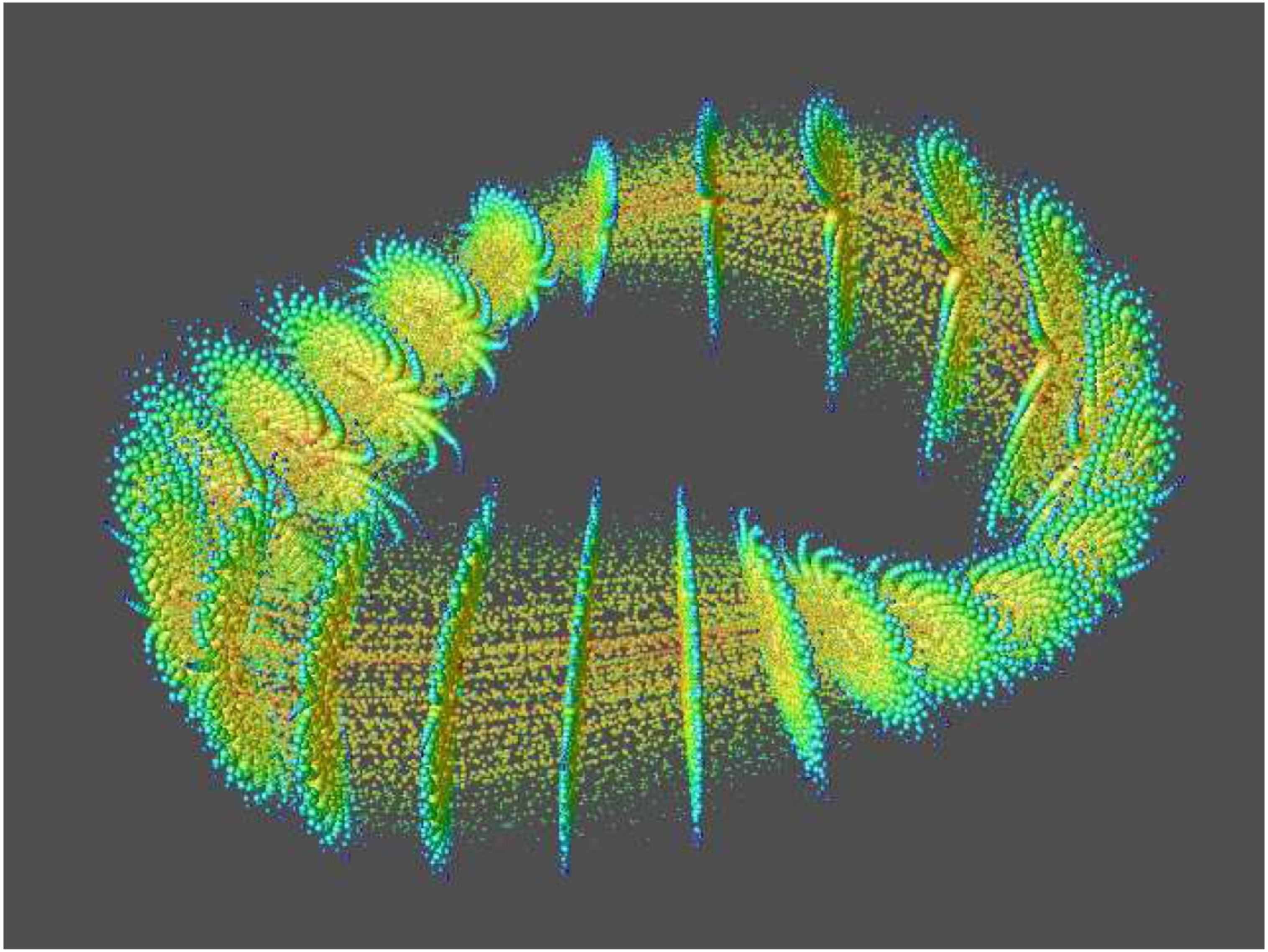

Platforms where VENUS is executed

- BlueGene/P (EPFL),
4096 quad-core nodes, 850 MHz, 56 Tops peak

- Cray XE-6 Monte Rosa (CSCS, Lugano),
1496 32-core nodes, 2.1 GHz, 402 Tops peak

- Bull HPC-FF (Juelich, Germany),
1080 8-core nodes, 2.93 GHz, 101 Tops peak

- IFERC – Helios (Rokkasho, Japan)
4410 16-core nodes, 2.70 GHz, 1.237 PF peak, Memory 256TB

VENUS/SCENIC codes used to predict techniques for controlling fusion plasmas

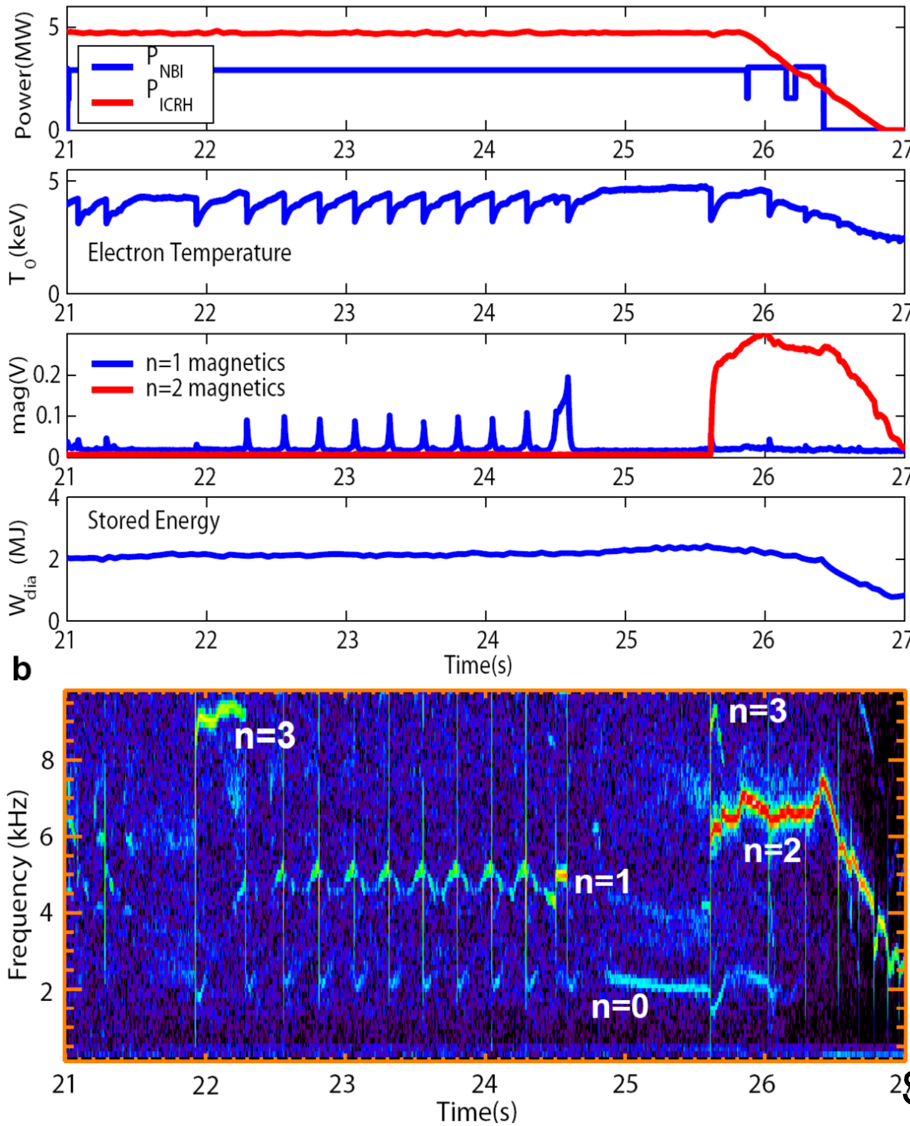

NBI and ICRH heating Required in order to obtained fusion grade plasmas

But we can get instabilities

Source: Graves, Nature Commun. 2012

VENUS/SCENIC codes used to predict techniques for controlling fusion plasmas

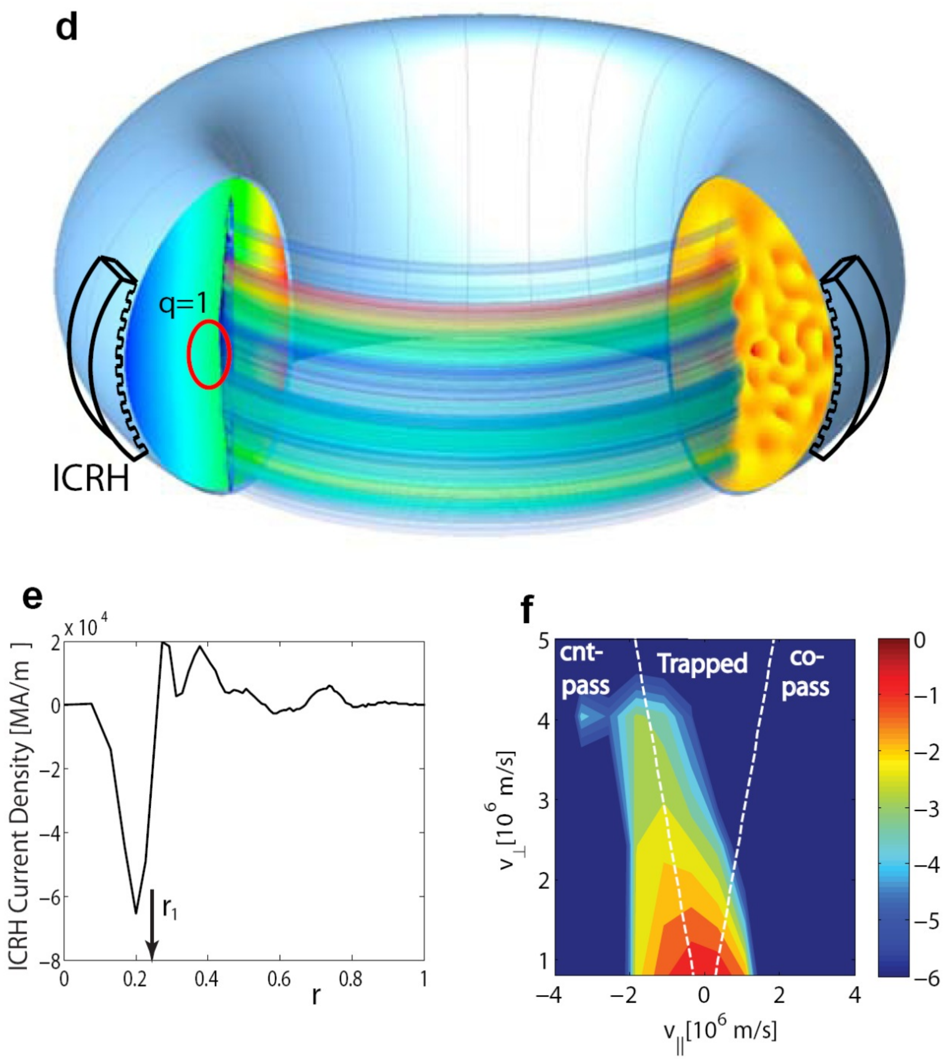

Modelling of the plasma tells us how to tune the ICRH Heating in order to avoid instability

Such phase space engineering is difficult. Parameter space too large for experimental study alone.

Modelling predictions enabled Massive step in control of Instability and improved plasma properties.

Source: Graves, Nature Commun. 2012

ICRH, fast particles in 3D tokamaks

- Investigation of ICRH deposition and fast particle confinement with SCENIC for the hybrid scenario proposed in ITER which could be susceptible to bifurcated helical core MHD equilibrium solutions

$v = 0$ $\qquad v = \pi/3$ $\qquad v = 2\pi/3$ $\qquad v = \pi$

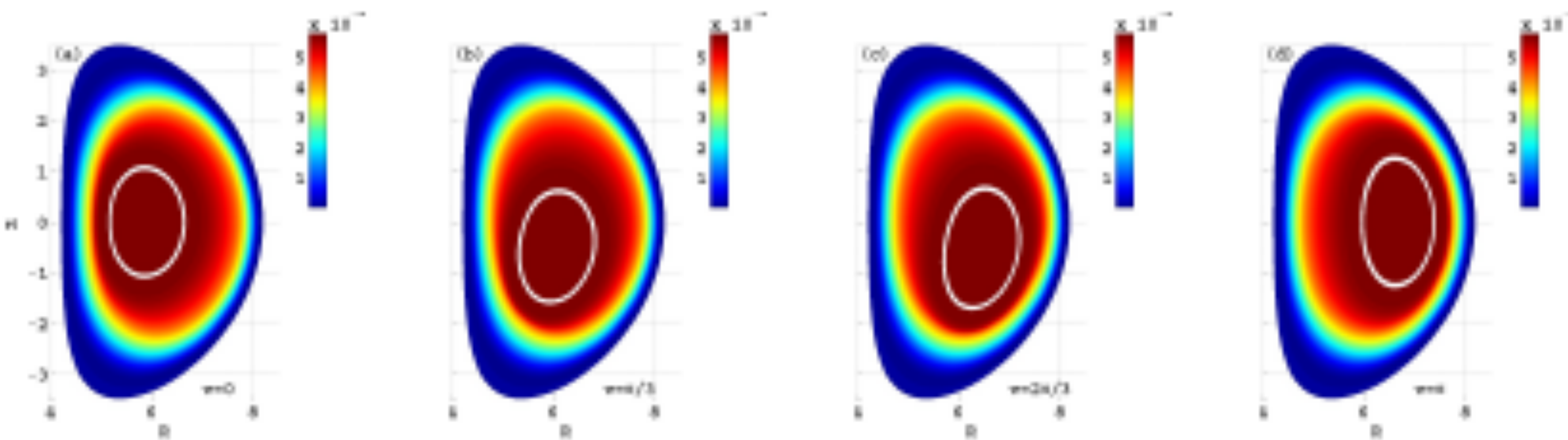

Summary

The SCENIC simulation package integrates an MHD equilibrium solver (ANIMEC), an ICRH wave propagation and absorption code (LEMan) and a guiding centre drift orbit particle code to obtain self-consistent anisotropic pressure MHD equilibrium states in conjunction with the ICRH wave power deposition and the fast ion distribution function in 2D and 3D geometry.

Applications in an axisymmetric JET tokamak configuration and a 3D quasi-axisymmetric stellarator have demonstrated converged solutions.

Due to intrinsic complexity, theoretical understanding of plasma dynamics relies on heavy computation. This is especially so for fast ion dynamics.

The CRPP at EPFL has developed a world leading modelling tool for fast ion populations and dynamics in fusion plasmas.

Simulations can be conveniently broken down into extremely efficiently parallelisable iterations.

Access to reliable machines, along with a professional support team has enabled high impact work to be undertaken.